Applied Catalysis B: Environmental 188 (2016) 123–133

Contents lists available at ScienceDirect

Applied Catalysis B: Environmental

journal homepage: www.elsevier.com/locate/apcatb

Selective catalytic reduction of NO by NH_3 with WO_3-TiO_2 catalysts: Influence of catalyst synthesis method

Yuanyuan He[a,b,1], Michael E. Ford[a], Minghui Zhu[a], Qingcai Liu[b], Zili Wu[c], Israel E. Wachs[a,*]

[a] Operando Molecular Spectroscopy & Catalysis Laboratory, Department of Chemical & Biomolecular Engineering, 7 Asa Drive, Lehigh University, Bethlehem, PA 18015, USA
[b] College of Materials Science and Engineering, Chongqing University, Chongqing, 400030, China
[c] Chemical Science Division and Center for Nanophase Materials Sciences, Oak Ridge National Laboratory, 1 Bethel Valley Road, Oak Ridge, TN 37831, USA

ARTICLE INFO

Article history:
Received 10 September 2015
Received in revised form 21 January 2016
Accepted 31 January 2016
Available online 2 February 2016

Keywords:
Catalysts
Co-precipitated
TiO_2
WO_3
Spectroscopy
Raman
IR
Temperature programmed surface reaction (TPSR)
Reaction
NO
NH_3
Selective catalytic reduction (SCR)

ABSTRACT

A series of supported WO_3/TiO_2 catalysts was prepared by a new synthesis procedure involving co-precipitation of an aqueous $TiO(OH)_2$ and $(NH_4)_{10}W_{12}O_{41}$*$5H_2O$ slurry under controlled pH conditions. The morphological properties, surface WO_x molecular structures, surface acidity and surface chemistry of the co-precipitated WO_3/TiO_2 catalysts were determined with BET, *in situ* Raman, *in situ* IR, steady-state $NO/NH_3/O_2$ SCR and NO/NH_3-temperature-programmed surface reaction (TPSR) spectroscopy, respectively. Time-resolved isotopic ^{18}O–^{16}O exchange with IR spectroscopy demonstrated that tungsten oxide was present as surface WO_x sites on the TiO_2 support with mono-oxo $O=WO_4$ coordination. In contrast to previous studies employing impregnation synthesis that found only surface one mono-oxo $O=WO_4$ site (1010–1016 cm^{-1}) on TiO_2, the co-precipitation procedure resulted in the formation of two distinct surface WO_x sites: mono-oxo $O=WO_4$ (~1012–1014 cm^{-1}) and a second mono-oxo $O=WO_4$ (~983–985 cm^{-1}). The new surface mono-oxo $O=WO_4$ (~983–985 cm^{-1}) site is thought to be associated with surface defects on the co-precipitated titania support. The co-precipitated catalysts exhibited slightly enhanced SCR reactivity that is thought to be related to the presence of the new surface $O=WO_4$ sites. Additional factors, however, may also be contributing. This is the first study that attempts to relate the molecular level structural properties of co-precipitated WO_3-TiO_2 catalysts with their surface reactivity for SCR.

1. Introduction

Supported tungsten oxide on titania catalysts possess both strong acid and modest redox characteristics resulting in their wide application for many reactions such as the selective catalytic reduction (SCR) of NO_x with NH_3 [1–3], various olefin conversion reactions [4–6] and photocatalytic decomposition of organic pollutants [7,8]. The supported WO_x/TiO_2 catalyst finds its greatest industrial use as an SCR catalyst because it exhibits excellent performance for the high temperature SCR process (300–400 °C) [9–12]. These catalytic properties have led to a significant number of studies that have examined the molecular structure, surface chemistry and performance of supported WO_x/TiO_2 catalysts [9–31].

Supported WO_x/TiO_2 catalysts are typically prepared by impregnation with aqueous solutions of tungstate salts (most commonly ammonium metatungstate) or grafting of tungsten alkoxides onto crystalline TiO_2 (anatase) supports [1,6–18]. Numerous synthesis procedures of supported WO_x/TiO_2 have also been reported by mechanical ball milling of physically mixed WO_3 and TiO_2 crystalline powders, [28,32], flame spraying of catalyst precursors [33] and grafting of tungsten(V) ethoxide onto TiO_2 [14,34]. The dispersion of tungsten oxide on the TiO_2 support was found to be higher from the chemical methods than the mechanical approach [28]. Deposition of tungsten oxide on TiO_2 results in a two-dimensional surface tungsten oxide layer on the TiO_2 support, with monolayer coverage corresponding to ~4.5 W atoms/nm^2, and higher amounts of tungsten oxide resulting in the additional formation of crystalline WO_3 nanoparticles (NPs) [23–26]. The dehydrated supported WO_x/TiO_2 catalysts also possess surface Brønsted and Lewis

* Corresponding author at: Department of Chemical & Biomolecular Engineering, Iaccoca Hall, 111 Research Drive, Lehigh University, Bethlehem, PA, 18015, USA.
E-mail address: iew0@lehigh.edu (I.E. Wachs).
[1] Present address: School of Electronic Information and Automation, Chongqing University of Technology, Chongqing 400030, China.

http://dx.doi.org/10.1016/j.apcatb.2016.01.072
0926-3373/

acid centers [21,22] associated with the surface mono-oxo O = WO_4 sites and only Lewis acid sites are present on the TiO_2 support [27].

Syntheses of supported WO_x/TiO_2 catalysts have also been reported from sol-gel methods [30,31] that employ aqueous titania precursors such as titanium oxyhydroxide or titanyl sulfate [30,31]. Co-precipitated WO_3-TiO_2 catalysts prepared from titanyl sulfate and ammonium paratungstate have been reported to possess improved thermal durability in comparison to the impregnated and grafted catalysts [2]. In contrast, it was concluded in other investigations that the choice of the TiO_2 precursor, titanium oxyhydroxide or TiO_2 powder, does not affect the development of the catalyst structure, surface acidity, or its catalytic performance for 2-propanol dehydration and *n*-hexane isomerization [29]. Some studies have proposed that the co-precipitated catalysts may also contain tungsten oxide in the titania interlayer spaces, but supporting evidence has not been provided [1,3,6]. Only one study has reported *in situ* Raman and IR spectra of dehydrated co-precipitated 15–20% WO_3-TiO_2 catalysts that exhibit a band at ~1015 cm^{-1} from surface WO_x species, typically present for conventional supported WO_x/TiO_2 catalysts, and a second band at ~980 cm^{-1}, which is not present for conventional supported WO_x/TiO_2 catalysts [15]. This study assigned the Raman bands to titania supported $(WO_x)_3$ clusters with the band at ~980 cm^{-1} resulting from W = O sites with predominantly W-O-Ti linkages to the titania support ("inner" sphere) and the band >1005 cm^{-1} associated with W = O sites from surface WO_x on top of the titania-supported tungsten oxide domains ("outer" sphere) [15]. Upon ^{18}O exchange with condensed $H_2{}^{18}O$, these bands shifted to 930 cm^{-1} and 961 cm^{-1}, respectively, which indicates that both bands indeed represent surface W = O oxo symmetric vibrations.

The nature of the tungsten oxide component present in co-precipitated WO_3-TiO_2 catalysts is becoming of greater interest in recent years since several industrial SCR catalyst patents have disclosed the synthesis of co-precipitated WO_3-TiO_2 catalysts with aqueous metatitanic acid ($TiO(OH)_2$) and tungsten oxide precursors [35–37]. These patents propose that at controlled alkaline pH values certain surface —OH hydroxyls form on the WO_3-TiO_2 powders that prevent aggregation of tungsten oxide on the TiO_2 support for the preparation scale employed for industrial production [36–38]. Fundamental studies on the nature of the tungsten oxide sites and surface chemistry of the co-precipitated WO_3-TiO_2 catalysts prepared under controlled aqueous pH values, however, have not been previously reported and should be of significant interest to both researchers and industrial practitioners. The use of such co-precipitated WO_3-TiO_2 catalysts as supports for surface vanadium oxide phases for SCR will be presented in a subsequent study, but it is important to first understand the nature of the co-precipitated WO_3-TiO_2 catalysts. Furthermore, V-free supported WO_x/TiO_2 catalysts are also sometimes employed in industry as SCR catalysts when minimization of SO_2 oxidation is desired [38].

In the present study, co-precipitated WO_3-TiO_2 catalysts have been synthesized from aqueous metatitanic acid and ammonium metatungstate under controlled aqueous pH conditions. The objective of the current study is to perform an in depth fundamental study of the influence of preparation parameters (pH value and calcination temperature) upon the final characteristics of the co-precipitated WO_3-TiO_2 catalysts and compare the findings with the properties of conventional supported WO_x/TiO_2 catalysts. Specific attention will be placed on the effect of these synthesis parameters on the co-precipitated WO_3-TiO_2 catalyst morphology (surface area and pore volume), tungsten oxide molecular structure(s) under dehydrated conditions (*in situ* Raman and IR spectroscopy), surface hydroxyls (*in situ* IR spectroscopy), surface acidity (*in situ* IR spectroscopy of chemisorbed ammonia) and catalytic activity for the $NO/NH_3/O_2$ SCR reaction.

2. Experimental

2.1. Catalyst synthesis

Metatitanic acid was precipitated from titanium isopropoxide ($Ti(O\text{-}i\text{-}Pr)_4$, Alfa Aesar, 99.999%) by addition of deionized water (molar ratio water/titanium isopropoxide = 110). After 60 min of stirring, the solution was filtered. The powder was washed with deionized water and finally dried at 120 °C for 6 h. The resulting powder was then added to the appropriate amount of deionized water to obtain a $TiO(OH)_2$ slurry with a concentration of 2 mol/L. Afterwards an aqueous solution (0.06 M) of ammonium metatungstate, $(NH_4)_{10}W_{12}O_{41}$, (Pfaltz & Bauer, 99.5% purity) was added to the $TiO(OH)_2$ suspension (5 wt% WO_3 in WO_3-TiO_2 powders) with stirring. Into this stirred suspension, a solution of concentrated aqueous ammonia (Fisher Scientific) was gradually added dropwise with continued stirring to obtain the desired pH value (5–10) to produce the co-precipitate gel. Water was removed from the gel by evaporation in a water bath. Each sample was dried at 120 °C overnight, and portions were calcined at 550, 600, 650 and 700 °C (heating rate 10 °C/min) for 4 h in an atmosphere of air. A conventional supported 5% WO_3/TiO_2 catalyst was also prepared by incipient wetness impregnation of aqueous ammonium metatungstate onto a TiO_2 (Degussa/Evonik, P-25, ~55 m^2/g, predominantly TiO_2(anatase) support for comparative purposes [16]. After drying at ambient temperature overnight, this catalyst sample was divided into four portions. The first was dried at 120 °C for 2 h and then calcined at 550 °C (heating rate 10 °C/min) for 4 h in an atmosphere of air. The remaining three were treated in the same way, with the exception that they were calcined at 600 °C, 650 °C, and 700 °C, respectively, for 4 h.

The WO_3/TiO_2 catalysts prepared by co-precipitation and incipient wetness impregnation are denoted as *a*WTi(C) pH*b*, and *a*WTi(I), respectively, where a represents the loading of WO_3(wt.%), (C) and (I) denote co-precipitation and incipient wetness impregnation respectively, and *b* indicates the pH value at which WOx was precipitated. For example, 5WT(C) pH10 means the WO_3/TiO_2 catalyst with a WO_3 loading of 5 wt.%, prepared by the co-precipitation method at pH10.

2.2. Catalyst characterization

2.2.1. BET- specific surface area measurement

BET surface areas were determined from adsorption-desorption isotherms of N_2 obtained at −196 °C using a Micromeritics ASAP 2020 apparatus. Typically, 0.200–0.300 g sample was used for each measurement. Each sample was outgassed under vacuum at 300 °C for 6 h prior to N_2 adsorption. The total pore volume, average pore diameters and pore size distributions were obtained from the N_2 adsorption branches of isotherms using the Barret–Joyner–Halenda (BJH) method.

2.2.2. X-ray diffraction (XRD) spectroscopy

XRD spectra were measured with a Rigaku Miniflex II diffractometer using Cu K-α radiation (1.5418 Å). Full scans of 5–90° (2-theta) were measured with a scan rate of 1°/min. The major peak scans of 23–26° (2-theta) were measured with a scan rate of 0.1°/min.

2.2.3. HS-LEIS

The outermost surface information was analyzed by a Qtac^{100} HS-LEIS spectrometer (ION-TOF) equipped with a highly sensitive double toroidal analyzer. The equipment provides 3000-fold higher sensitivity than conventional LEIS spectrometers, allowing for quantitative static depth profiling. Prior to the measurements, the samples were dehydrated in static O_2 at 0.2 bar and 400 °C for

1 h in a preparation chamber connected to the spectrometer. After dehydration, the preparation chamber was evacuated and the samples were directly transferred to the main UHV chamber for the measurements. The HS-LEIS spectra were collected using 1.0 KeV He^+ as ion sources. For depth profiling, the surface was sputtered with 3.0 KeV Ar^+, each sputter and measurement cycle yield of 1×10^{15} ions/cm^2 corresponding to ~1 surface layer (0.2 nm).

2.2.4. Raman spectroscopy

Raman spectra were obtained with visible (532 nm) laser excitation on a single stage Horiba-Jobin Yvon Laboratory Ram-HR Raman spectrometer with a confocal microscope (Olympus BX-30), notch filter (Kaiser Super Notch), and a 900 groves/mm grating. The visible laser excitation was generated with Nd-YAG double diode pumped laser (Coherent Compass 315M-150, output power of 150 mW with sample power 10 mW). The scattered photons were directed into a single monochromator and focused onto a UV-sensitive LN_2 cooled CCD detector (Horiba-Jobin Yvon CCD-3000 V) with a spectral resolution of ~2 cm^{-1} for the given parameters. The notch filter has a ~100 cm^{-1} cutoff for visible spectra; Raman spectra were collected above 200 cm^{-1}. The catalysts were dehydrated in an environmental cell (Linkam CCR1000) in flowing 10% O_2/Ar (Airgas, 10%O_2/Ar, 25 mL/min) at 450 °C for 1 h, and then cooled under flowing 10% O_2/Ar to 120 °C to ensure that the catalyst surface was void of moisture before spectra were collected. Spectral collection times were typically 30 s per scan with five scans.

2.2.5. Infrared spectroscopy

In situ IR experiments were performed on a Thermo Nicolet 8700 FTIR spectrometer equipped with a Harrick Praying Mantis Attachment (model DRA-2) for diffuse reflectance spectroscopy and a high sensitive mercury-cadmium-telluride (MCT-A) detector. Powder samples were loaded into an environmental cell (Harrick, HVC-DRP-4) connected to a purging and adsorption gas control system. The temperature of the reaction chamber was controlled by a Harrick ATC Temperature Controller.

Catalysts were dehydrated by heating to 450 °C for 1 h under flowing 10% O_2/Ar (30 mL/min; heating rate of 10 °C/min). IR spectra of the dehydrated samples were collected after cooling the catalysts to 110 °C under flowing 10% O_2/Ar. Subsequently at 110 °C, 10% O_2/Ar was replaced by flowing Ar (30 mL/min; 20 min) and then by flowing 1.5% NH_3/He (30 mL/min; 30 min). Physisorbed NH_3 was removed by flowing Ar (30 mL/min; 30 min). For SCR reactions with NO, Ar was replaced by flowing 2000 ppm NO/He (30 mL/min) and the catalyst was heated to 450 °C at 5 °C/min. In both instances, IR spectra were recorded at 50 °C intervals.

For the $H_2{}^{18}O$ exchange experiment, IR spectra were collected with a Thermo Nicolet Nexus 670 spectrometer equipped with a diffuse reflectance cell (HC-900, Pike Technologies). The WO_x/TiO_2 sample was pretreated in flowing 5% O_2/He (25 mL/min) at 450 °C for 1 h. An IR spectrum of the unexchanged catalyst was collected after cooling to 120 °C in flowing He (25 mL/min). The sample was then heated to 400 °C under flowing He (25 mL/min). A background spectrum was obtained before the sample was exposed to $H_2{}^{18}O$/He (15 mL/min He bubbling through a $H_2{}^{18}O$ saturator at room temperature) at 400 °C for 1 h. Time-resolved spectra were collected during the exchange at 400 °C. After cooling to 120 °C under flowing He (25 mL/min), the spectrum of the exchanged catalyst was collected.

For comparisons, IR spectra were normalized using the TiO_2 band at ~800 cm^{-1} prior to integration.

To evaluate the relative amounts of surface O = WO_4 functionality and the new WO_x species, the IR spectra of the overtone region were deconvoluted and integrated after subtraction of a linear background using CasaXPS® software.

2.2.6. Temperature-Programmed surface reaction (TPSR) spectroscopy

The surface chemistry and reactivity of the supported tungsten oxide catalysts were chemically probed by NH_3 TPSR spectroscopy, using an Altamira AMI-200 spectroscope equipped with a Dycor Dymaxion DME200MS online quadrupole mass spectrometer. Typically, ~160 mg of catalyst was loaded into a U-type quartz tube and initially treated in flowing 10%O_2/Ar to 480 °C (30 mL/min; heating rate of 10 °C/min) for 60 min to remove any possible adsorbed organic impurities and to dehydrate the sample. To ensure that the surface MO_x species remained in the fully oxidized state, the pretreated samples were cooled to 60 °C under flowing 10% O_2/Ar at which time the gas stream was switched to Ar (Airgas, ultra-high purity. 30 mL/min) and held for 30 min to flush out any residual gas-phase O_2 and to remove any physically adsorbed O_2 and background gases. After O_2 treatment, two different experiments were performed. For first type of experiment, ammonia adsorption was performed by flowing 2000 ppm NH_3/He (Airgas, 30 mL/min) at 60 °C for 30 min, then the system was purged with flowing Ar (Airgas, ultra high purity. 30 mL/min) for another 30 min to remove any physically adsorbed ammonia. The gas stream was then switched to 2000 ppm NO/He (Airgas, 30 mL/min). After flowing 2000 ppm NO/He (with 5% O_2/He) for 10 min at 60 °C, the sample was heated at a constant heating rate (5 °C/min) to 480 °C and held at 480 °C for 30 min. For the second type of experiment, a mixture of NO, NH_3, O_2 and He was introduced into the reactor with NO:NH_3:O_2 = 7:7:25 at 60 °C, and then the sample was heated to 500 °C at 10 °C/min.

The gases exiting the quartz tube reactor were analyzed with the online mass spectrometer as a function of catalyst temperature. The following *m/e* ratios were employed for the identification of the desorption gases: O_2, *m/e* = 32; N_2, *m/e* = 28; H_2O, *m/e* = 18; NH_3, *m/e* = 17; NO, *m/e* = 30; N_2O, *m/e* = 44; and NO_2, *m/e* = 46. Results for NH_3 were corrected by subtraction of the contribution to the m/e = 17 peak by the mass spectrum of water.

2.2.7. Steady-State SCR reaction

The steady-state SCR reaction was performed on an Altamira AMI-200 spectroscope equipped with a Dycor Dymaxion DME200MS online quadrupole mass spectrometer. About 30 mg of catalyst was loaded into a U-type quartz tube for the reaction studies. Initially the catalyst was treated with 10% O_2/Ar at 500 °C for 1 h to remove any possible adsorbed organic impurities, adsorbed moisture and to ensure that the surface MO_x species are in the fully oxidized state. Then the system was flushed with He for 10 min, after which a reaction mixture was introduced (35 mL/min 2000 ppm NH_3/He, 35 mL/min 2000 ppm NO/He, 5 mL/min 5% O_2/He and 5 mL/min Ar). The SCR reaction was performed at 3 different temperatures for 2 h at each temperature to ensure that steady-state reaction conditions were achieved. The gases exiting the quartz tubular reactor were analyzed with the online mass spectrometer. The following *m/e* ratios were employed for the identification of the exiting gases: O_2, *m/e* = 32; N_2, *m/e* = 28; NH_3, *m/e* = 17; NO, *m/e* = 30.

3. Results

3.1. Physical and morphological properties (texture of catalysts)

The synthesis conditions for the co-precipitated WO_3-TiO_2 catalysts were found to influence the specific surface area, BJH adsorption pore volume, average pore diameter and surface W density of the catalysts calcined at 550 °C. As summarized in Table 1, the co-precipitated 5% WO_3-TiO_2 catalysts prepared under acidic and neutral pH values (pH 5–8) possess slightly higher specific surface areas (82–88 m^2/g), greater pore volumes (0.20–0.22 cm^3/g),

Table 1
BET surface area, Barrett Joiner Halenda (BJH) pore volume, and pore distribution for the co-precipitated WO_3-TiO_2 catalysts, the incipient wetness model analog and P-25 support.

Preparation pH	Calcination temp (°C)	Surface area (m^2/g)	W density (atoms/nm^2)	Pore volume (cm^3/g)	Pore size (nm)
5	550	85	1.5	0.20	8.5
6	550	88	1.8	0.22	9.1
7	550	82	1.6	0.20	8.7
8	550	84	1.5	0.20	8.5
9	550	57	2.3	0.16	8.6
10	550	66	2.0	0.14	7.6
5	700	39	3.3	0.16	15.4
10	700	36	3.6	0.13	14.0
P25	550	48	–	0.19	9.7
P25	700	19	–	0.15	31.4
Incipient wetness – P25	550	53	2.4	0.43	30.2
Incipient wetness – P25	700	41	3.2	0.40	38.2

larger pores (8.5–9.1 nm) and, consequently, lower surface W density on the TiO_2 support (1.5–1.6 W atoms/nm^2). In contrast, the co-precipitated 5% WO_3-TiO_2 catalysts prepared under alkaline condition (pH 9–10), possess slightly lower specific areas (57–66 m^2/g), smaller pore volumes (0.14–0.16 cm^3/g), smaller pores (7.6–8.6 nm), and higher surface W density on the TiO_2 support (2.0–2.3 W atoms/nm^2). The 7.6–9.1 nm pore size distribution indicates that the catalysts primarily consist of mesopores. The surface area and pore volume values decrease with increasing calcination temperature while the pore size becomes larger. The differences between the 5% WO_3-TiO_2 samples prepared at low and high pH values are minimized with increasing calcination temperature. Although large pore volumes are beneficial in minimizing mass transfer limitations, the corresponding higher surface areas and larger pore diameters can also lead to greater catalyst deactivation from sintering of the co-precipitated WO_3-TiO_2 catalysts [3].

The model supported 5% WO_x/TiO_2 catalyst prepared by incipient wetness possesses a large pore volume (0.43 cm^3/g) and pores (~30 nm) with modest surface area (53 m^2/g) giving a higher surface W density on the TiO_2 support (2.4 W atoms/nm^2). Calcination at elevated temperatures doesn't seem to perturb the pore volume, modestly decreases the surface area (41 m^2/g) and further increases the pore diameter (~38 nm) and surface W density on the TiO_2 support (3.2 W atoms/nm^2). Although the high temperature calcination results in comparable surface area values for all the catalysts, the model supported WO_x/TiO_2 catalyst retains its much greater pore volume and pore diameter compared to the co-precipitated catalysts. In the absence of WO_x, the model TiO_2 support (P25) significantly decreases its BET surface area from 48 to 19 m^2/g when the calcination temperature is increased from 550 to 700 °C, respectively. This behavior reflects the stabilization induced by the surface WO_x sites on the thermal stability of the TiO_2 support.

3.2. XRD and HS-LEIS

The XRD diffractograms are given in Figs. S1 and S2 and reveal that TiO_2(P-25)-containing catalysts mainly consist of the anatase phase, but also contain some rutile phase. The co-precipitated TiO_2(C)-containing catalysts are also dominated by the anatase phase without rutile, but also possess some brookite and $H_2Ti_3O_7$. The constant position of the TiO_2(anatase) XRD peaks for the co-precipitated catalysts reveals that there is no evidence for formation of W-Ti oxide solid solutions. HS-LEIS surface analysis confirms that the W/Ti ratios are essentially the same for the co-precipitated and model impregnated catalysts indicating surface segregation of the W oxides on the titania support (Fig. S3). Depth profiling of both P-25 supported and co-precipitated WTi catalysts showed that the values of the W/Ti ratios decreased smoothly from ~1.0 at 0.1 nm depth to ~0.5 at 0.8 nm consistent with surface segregation of W oxides. The much broader XRD peaks for the co-precipitated catalysts reflect the smaller particles and/or greater disorder of the co-precipitated catalysts relative to the impregnated catalysts (Table S1).

3.3. In situ *Raman spectroscopy*

3.3.1. *Nature of tungsten oxide species*

The Raman spectra of the dehydrated co-precipitated WO_3-TiO_2 and model supported WO_3/TiO_2 catalysts (550 °C) are presented in Fig. 1. The TiO_2 (anatase) support gives rise to a weak second-order feature at ~795 cm^{-1}. [39] The absence of a Raman band at ~805 cm^{-1} indicates that crystalline WO_3 nanoparticles (NPs) are not present and the tungsten oxide phase is completely dispersed for the co-precipitated WO_3-TiO_2 and model supported WO_x/TiO_2 catalysts [33,40]. The model supported WO_x/TiO_2 catalyst exhibits only one tungsten oxide band at ~1016 cm^{-1} that has been assigned to the symmetric stretch of the surface mono-oxo O = WO_4 species [41–43]. It was previously shown that the Raman band for the surface WO_x species on TiO_2 shifts from ~1007 to ~1016 cm^{-1} as the surface WO_x species oligomerize with increasing surface coverage on TiO_2, which indicates that the model catalyst possesses an extensively oligomerized surface WO_x species [23]. The co-precipitated WO_3-TiO_2 catalysts display a similar Raman band at ~1012–1014 cm^{-1}, the symmetric stretching mode of the surface polytungstate mono-oxo O = WO_4 species, which qualitatively tracks the surface W density on TiO_2 (see Table 1) [41–43]. The slight shift from 1012 to 1014 cm^{-1} suggests that the surface WO_x species slightly oligomerize on TiO_2 with decreasing pH values during synthesis. A new weak Raman band from a second WO_x site at ~983–985 cm^{-1} also appears; this new band is not present in the model supported WO_x/TiO_2 catalyst. The molecular structural assignment of the new WO_x species giving rise to the Raman band at ~983–985 cm^{-1} requires additional characterization information and will be addressed below in the discussion section.

3.3.2. *Thermal stability of WO_3-TiO_2 catalysts*

The influence of calcination temperature, 550–700 °C, on the dehydrated co-precipitated WO_3-TiO_2 catalyst prepared with a solution pH = 8 is shown in the series of *in situ* Raman spectra of Fig. S4. The shift of the symmetric W = O vibration from ~1013 to ~1018 cm^{-1} with increasing calcination temperature reflects the formation of longer surface O = WO_4 oligomers [44]. The higher calcination temperatures do not result in the appearance of TiO_2 (rutile) (Raman bands at 142, 445 and 610 cm^{-1}) [45] or crystalline WO_3 NPs (Raman band at ~805 cm^{-1}) [13,16,23,46–48]. The Raman spectra indicate the thermal stability of the TiO_2 (anatase) support, the new WO_x species and the surface polytungstate mono-oxo O = WO_4 species with higher calcination temperature. The thermal stability of the co-precipitated WO_3-TiO_2 catalysts indicates

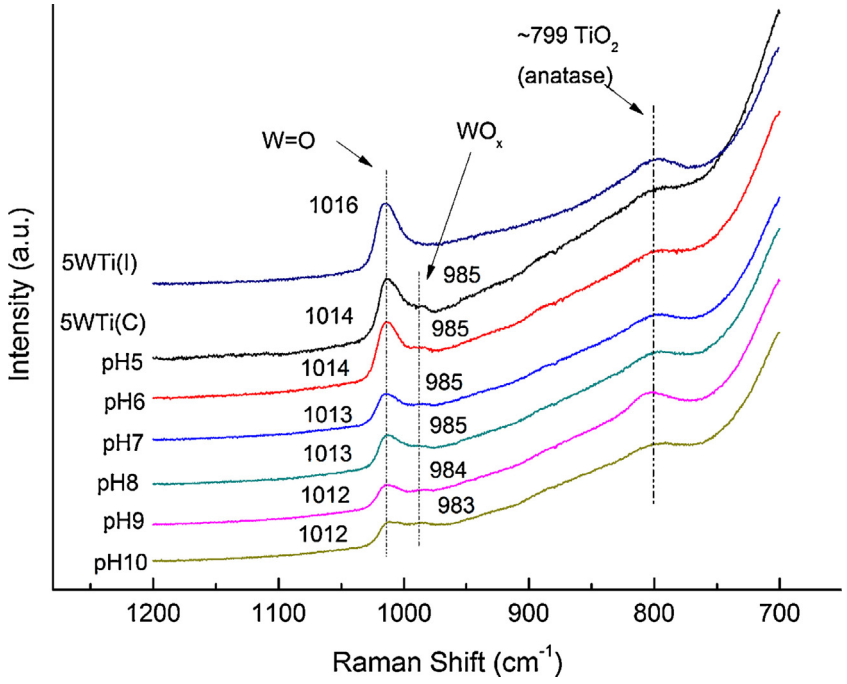

Fig. 1. *In situ* Raman (532 nm) spectra of dehydrated co-precipitated 5% WO_3-TiO_2 catalysts (pH 5–10, calcined at 550 °C) and model supported 5% WO_x/TiO_2 catalyst (550 °C).

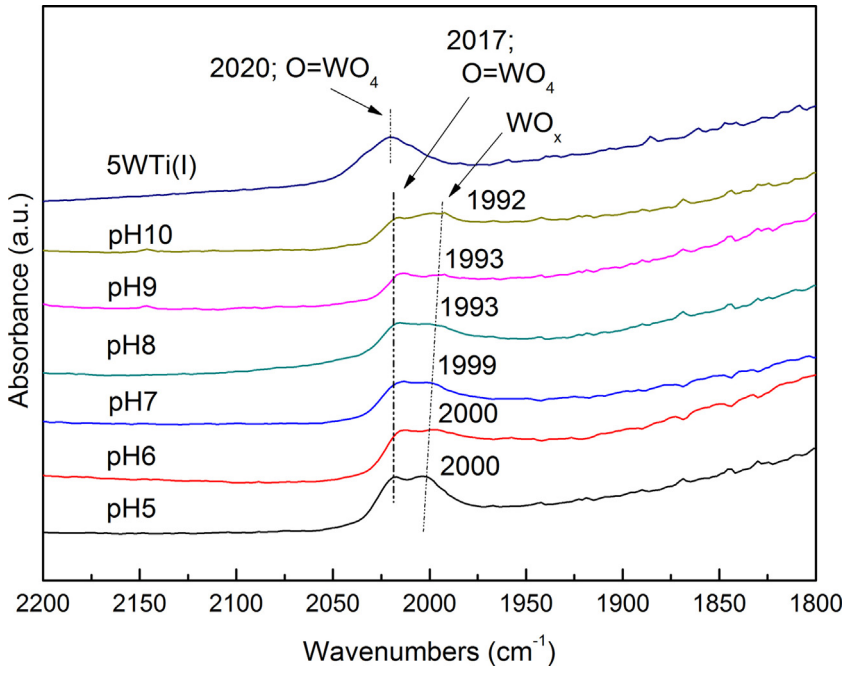

Fig. 2. *In situ* IR spectra of the overtone region of dehydrated co-precipitated 5% WO_3-TiO_2 (pH 5–10, 550 °C) and model supported 5% WO_x/TiO_2 catalyst (550 °C). Spectra collected after cooling the catalysts to 110 °C under flowing 10% O_2/Ar.

the stabilizing influence of the dispersed tungsten oxide species upon the TiO_2 (anatase) support [32]. Similar results were also found for the other co-precipitated WO_3-TiO_2 catalysts prepared at different solution pH values and their Raman spectra with calcination temperature are omitted for brevity. The model supported WO_x/TiO_2 catalyst was also found to be thermally stable indicating that the surface polytungstate species impart thermal stability as well to this TiO_2 (anatase) support. The Raman shift from ~1010 to ~1016 cm^{-1} of the W = O vibration also reflects oligomerization of the surface WO_x species as the TiO_2 surface area decreased from the 700 °C calcination treatment [23]. Such vibrational red shifts are related to the increasing dipole–dipole coupling between W = O oscillators in surface tungsten oxide species with higher degrees of polymerization [23,49].

3.4. In situ *IR spectroscopy*

3.4.1. *Nature of tungsten oxide species*

The *in situ* IR spectra of the overtone region of the dehydrated co-precipitated WO_3-TiO_2 and model supported WO_x/TiO_2 catalysts (550 °C) are depicted in Fig. 2. Strong IR absorption by the TiO_2 support between 700 and 1050 cm^{-1} prevents detection of the pri-

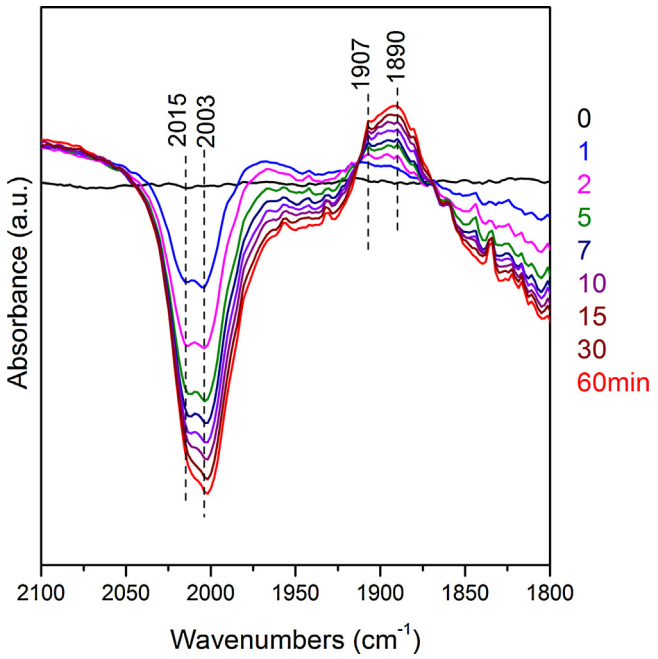

Fig. 3. Time-resolved *in situ* IR difference spectra of dehydrated co-precipitated 5% WO_3-TiO_2 catalysts (pH 5, calcined at 550 °C) collected during isotopic exchange with $H_2{}^{18}O_2$ at 400 °C. Negative absorbance indicates bands corresponding to species consumed and positive bands result from new species formed.

mary vibrations of the surface polytungstate mono-oxo O = WO_4 and new WO_x species in the 980–1020 cm^{-1} region [50–52]. Fortunately, the overtone vibrations of the tungstate species can be detected with IR spectroscopy in the 1950–2050 cm^{-1} range [51,52]. The model supported WO_x/TiO_2 catalyst containing only surface polytungstate mono-oxo O = WO_4 species exhibits only one overtone band at ~2015 cm^{-1} as expected for a mono-oxo tungstate structure from vibrational spectroscopy selection rules [52]. The co-precipitated WO_3-TiO_2 catalysts, however, exhibit two weak IR overtone bands at ~2017 and ~1992–2000 cm^{-1} corresponding to the vibrations of the surface polytungstate mono-oxo O = WO_4 and new WO_x species, respectively. The relative ratio of the new WO_x species/surface polytungstate mono-oxo O = WO_4 species increases as the preparation pH increases (Fig. S5) suggesting that these vibrations originate from two distinct tungsten oxide sites.

3.4.2. Time-resolved in situ IR ^{18}O-^{16}O exchange

Additional information about the nature of the WO_x sites in the co-precipitated WO_3-TiO_2 catalysts can be provided by time-resolved IR ^{18}O–^{16}O exchange presented in Fig. 3. The rapid decrease of ^{16}O-containing vibrations (~2000–2015 cm^{-1}) and formation of ^{18}O-containing vibrations (~1890–1910 cm^{-1}) demonstrate that both tungsten oxide sites are present as surface species since bulk WO_x sites in the titania lattice would require longer exchange times. For example, the TiO_2 Raman vibrations (anatase: 398, 518, 642, and 796 cm^{-1}; trace of brookite: 324 cm^{-1}) [53] are minimally perturbed by the ^{18}O–^{16}O exchange process even after 60 min while a majority of the WO_x sites become exchanged (~70%) after 60 min (compare Figs. S6 and S7). This indicates that almost all of the tungsten oxide in co-precipitated catalysts is present on the surface and not trapped in the TiO_2 bulk lattice during calcination. Furthermore, the ^{18}O–^{16}O exchange reveals that both tungsten oxide sites possess mono-oxo O = WO_4 coordination since dioxo $(O=)_2WO_2$ sites would also give rise to strong $^{18}O=W=^{16}O$ vibrations at ~1925–1975 cm^{-1} that are absent from the IR spectra [54].

Table 2
IR analysis of surface Brønsted (1419 cm^{-1}) and Lewis acid (1603 cm^{-1}) sites on WO_x-TiO_2 catalysts probed with ammonia adsorption at 100 °C.

Preparation pH [Calcination temp (°C)]	Ratio of B/L sites	Ratio of Bronsted (1419 cm^{-1}) sites/TiO_2 (~800 cm^{-1}) x 10^2	Ratio of Lewis (1603 cm^{-1}) sites/TiO_2 (~800 cm^{-1}) x 10^2
5 (550)	1.3	4.7	3.7
6 (550)	1.0	4.8	4.7
7 (550)	1.1	4.9	4.3
8 (550)	0.9	3.6	3.7
9 (550)	0.8	3.4	4.3
10 (550)	0.7	3.1	4.6
Incip. wetness on P25(550)	1.2	3.3	4.0
5 (700)	3.0	5.0	1.7

3.4.3. Surface acidity

The surface acidity of supported WO_3/TiO_2 catalysts is known to significantly impact the NO/NH_3 SCR reaction and is typically chemically probed with chemisorption of basic NH_3 [55–57]. *In situ* IR spectra after chemisorption of ammonia on the series of dehydrated co-precipitated WO_3-TiO_2 and the model impregnated 5% WO_x/TiO_2 catalysts are presented in Fig. 4. Chemisorption of ammonia on the co-precipitated WO_3-TiO_2 and model supported WO_x/TiO_2 (A) catalysts significantly diminishes the IR vibrations from the surface hydroxyls and reflects the direct interaction of adsorbed ammonia with the surface hydroxyls. The IR bands at 1180 and 1603 cm^{-1} correspond to the symmetric and asymmetric bending vibrations, respectively, of surface $NH_3{}^*$ chemisorbed on Lewis acid sites [55–59]. The IR band at 1419 cm^{-1} corresponds to the asymmetric bending vibration of surface $NH_4{}^{+*}$ chemisorbed on Brønsted acid sites [55–59]. The corresponding symmetric bending vibration of chemisorbed $NH_4{}^{+*}$ appears as a weak shoulder at 1660 cm^{-1}. The vibrations of the surface $NH_3{}^*$ and $NH_4{}^{+*}$ species are independent of the different pH values employed during the synthesis, which indicates that similar surface acid sites are present for all the catalysts. Surface $NH_3{}^*$ species bound to Lewis acid sites also vibrate at 3161 and 3257 cm^{-1} (ν_s $NH_3{}^*$) and 3346/3382 cm^{-1} ($_{as}$ $NH_3{}^*$) [55]. The band at 3571 cm^{-1} is from the N—H stretch of adsorbed ammonia. The model impregnated supported WO_x/TiO_2 catalyst also possesses the same IR bands for chemisorbed ammonia. Vibrations from surface NH* (3200 cm^{-1}) [60] and surface $NH_2{}^*$ (ν_{as} and $_s$ at 3380 and 3290 cm^{-1}, respectively) [60] are not detected suggesting that the surface NH* and $NH_2{}^*$ intermediates are either not present, present in concentrations too low to be detected with IR, or not IR active.

To assess the relative concentrations of the surface Brønsted and Lewis acid sites in the WO_3-TiO_2 catalysts, the IR bands were integrated (1419 cm^{-1} for Brønsted acid sites and 1603 cm^{-1} for Lewis acid sites) and normalized against the TiO_2 band at ~800 cm^{-1} internal standard (see Table 2). The IR bands indicate that the amount of Brønsted acid sites decreases as the synthesis pH is increased while the Lewis acid sites show an opposite trend with synthesis pH for the co-precipitated catalysts. The acid properties of the model supported 5% WO_x/TiO_2 catalyst most closely approach that of the co-precipitated catalyst synthesized at a pH of 10. With one exception, the ratio of Brønsted/Lewis acid sites of the co-precipitated catalysts is slightly lower than that of model incipient wetness analog catalyst (5WTi(I)). Upon calcination of the co-precipitated catalysts at 700 °C, the amount of Brønsted acid sites slightly increases, but the amount of Lewis acid sites significantly decreases. These changes result in a much higher Brønsted/Lewis ratio of surface acid sites upon calcination at 700 °C.

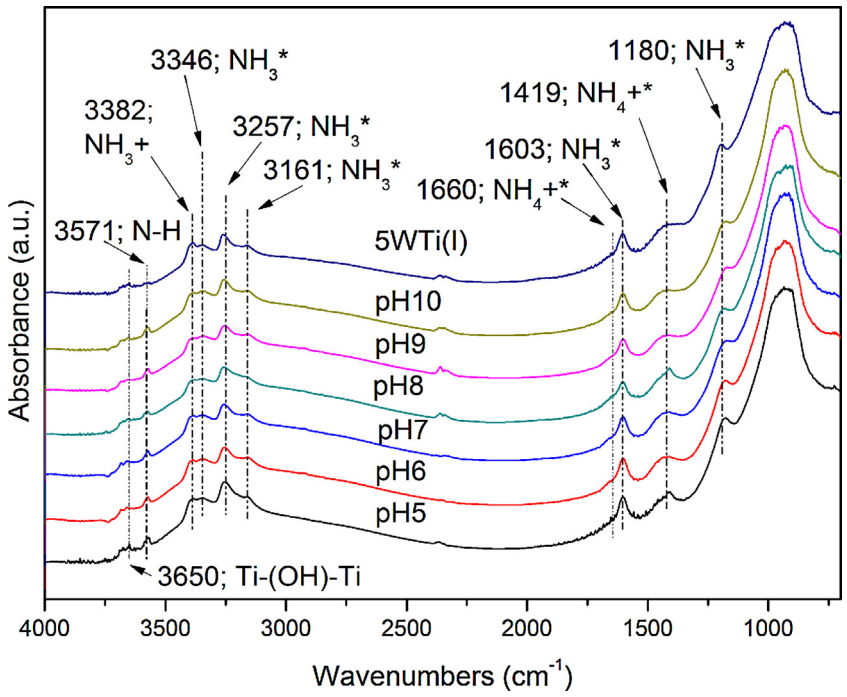

Fig. 4. *In situ* IR spectra of NH_3 adsorption over the series of co-precipitated 5% WO_3-TiO_2 catalysts (pH 5–10 and 550 °C) and impregnated model supported 5% WO_x/TiO_2 catalyst. Spectra collected after cooling the catalysts to 110 °C under flowing 10% O_2/Ar.

3.5. $NO/NH_3/O_2$ SCR-temperature programmed surface reaction (TPSR) spectroscopy

The surface chemistry of the supported WO_x sites on the TiO_2 supports was probed with temperature programmed $NO/NH_3/O_2$ SCR. All the WO_x-TiO_2 catalysts initiate the SCR reaction at ~325 °C. As the temperature is increased, the activity differences between the catalysts become more apparent: 5WTi(C) pH 10 » 5WTi(C) pH 5 > 5WTi(I) (Fig. 5). Probing the surface chemistry of the WO_x-TiO_2 catalyst by first chemisorbing a monolayer of ammonia and performing TPSR in flowing NO/Ar (see Fig. S8) reveals two N_2 formation peaks for N_2 evolution at ~340 and 430 °C for all the catalysts. All the catalysts exhibit the same amount of N_2 formation at 430 °C, but the amount of evolved N_2 at 340 °C is a function of the specific catalyst: 5WTi(C) pH 10 » 5WTi(C) pH 5 > 5WTi(I). The TPSR experiment reveals that the co-precipitated catalyst has a greater number of the more active sites responsible for N_2 evolution at 340 °C, especially the 5WTi(C) pH 10 catalyst. The ability to perform the lower temperature NO/NH_3 SCR reaction in the absence of gas phase molecular O_2 indicates that this reaction is able to proceed with redox lattice oxygen from the catalyst, presumably from the surface WO_x sites.

Unreacted surface ammonia also desorbs during the NO/NH_3-TPSR from ~100–400 °C. The amount of desorbed NH_3 is comparable for the co-precipitated catalysts (Fig. S9). The greater N_2 and NH_3 evolution from the 5WTi(C) pH 5 and 5WTi(C) pH 10 catalysts during NO/NH_3 SCR-TPSR indicates that the co-precipitated catalysts have greater capacities for NH_3 adsorption than the model supported 5WTi(I) catalyst. The amount of desorbed NH_3 does not track the BET surface areas of the catalysts since the surface area of the 5WTi(C) pH10 catalyst (66 m^2/g) is lower than that of 5WTi(C) pH 5 (85 m^2/g) with the former evolving more N_2. This suggests that the nature of the surface sites of the WO_x-TiO_2 catalysts impacts the catalyst capacity for ammonia adsorption.

Table 3
Turnover Frequency (TOF) of co-precipitated 5WTi(C) (pH = 10, 550 °C) and impregnated supported 5WTi(I) (550 °C) catalysts at 360 °C.

Catalyst	Ns mol/g	Reaction Rate mol/g.s	TOF s^{-1}
5WTi(I)	2.2E-04	1.3E-07	6.2E-04
5WTi(C) pH5	2.2E-04	1.6E-07	7.3E-04
5WTi(C) pH10	2.2E-04	2.2E-07	1.0E-03

3.6. Steady-state $NO/NH_3/O_2$ SCR reaction

The steady-state reaction rates, TOF and activation energy values of the $NO/NH_3/O_2$ SCR reaction at 360 °C by the co-precipitated and model impregnated WO_x/TiO_2 catalysts are presented in Fig. 6 and Table 3. The co-precipitated 5WTi(C) pH 10 catalyst is the most active followed by the 5WTi(C) pH 5 catalyst that is slightly more active than the model 5WTi(I) catalyst. The apparent activation energy values for the co-precipitated catalysts are comparable (~82 kJ/mol) and lower than the apparent activation energy for the model impregnated 5WTi(I) catalyst (~91 kJ/mol).

4. Discussion

4.1. Molecular structures of titania-supported tungsten oxide phases

The dehydrated co-precipitated 5% WO_3-TiO_2 catalysts possess two distinct surface tungsten oxide sites, with Raman bands at ~1012-1014 and ~983–985 cm^{-1}. The Raman band at 1012–1015 cm^{-1} (overtone IR band at ~2017 cm^{-1}) corresponds to the symmetric stretch of dehydrated surface mono-oxo $O=WO_4$ species anchored at basic surface TiOH sites as seen for the model supported 5% WO_x/TiO_2 impregnated catalyst [16,17,51,52]. The second Raman band at ~983–986 cm^{-1} (overtone IR band at ~1992–2003 cm^{-1}) also originates from surface WO_x sites, as demonstrated by the rapid isotopic oxygen exchange, and

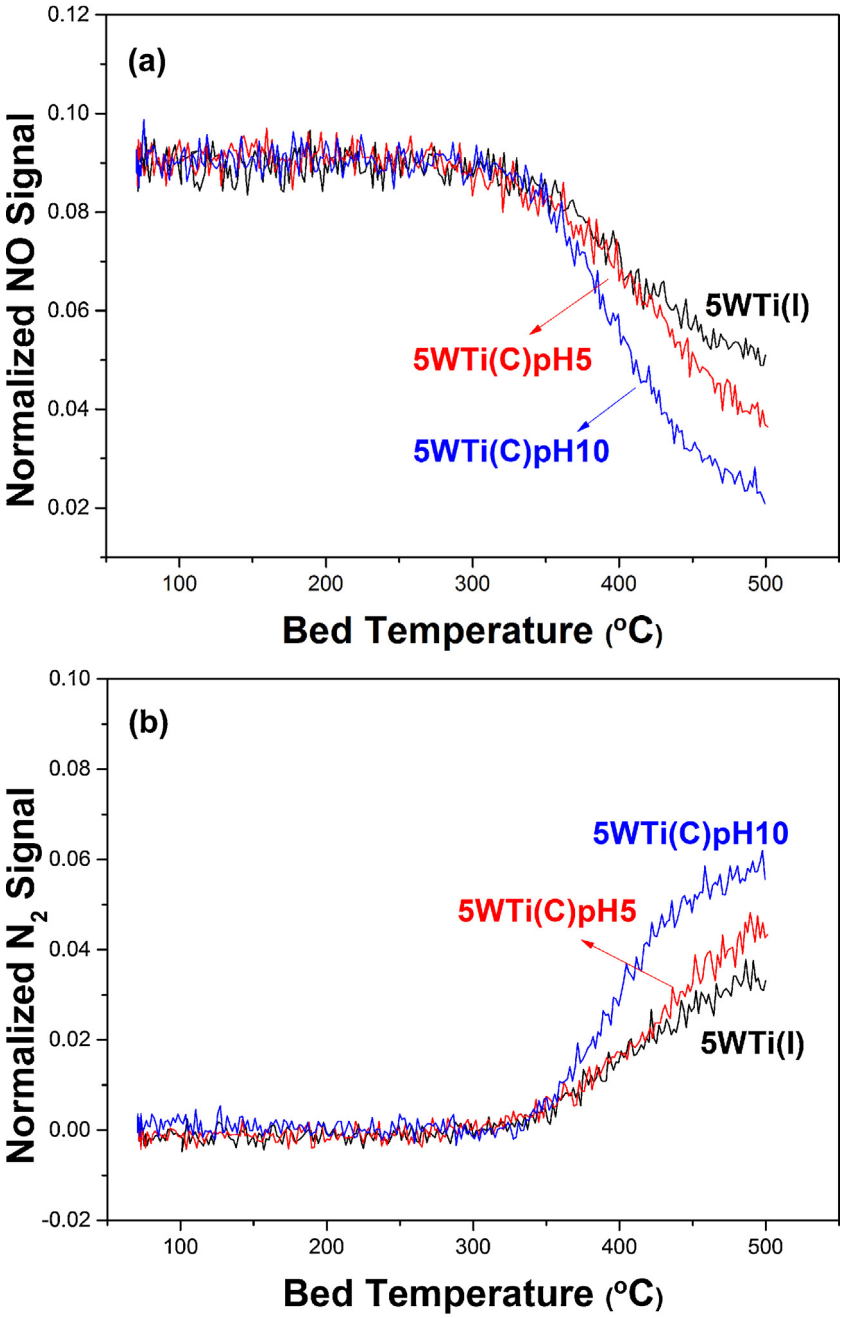

Fig. 5. Consumption of NO (a) and evolution of N_2 (b) during temperature programmed $NO/NH_3/O_2$ SCR for the co-precipitated 5WTi(C)(pH 5, 550 °C), co-precipitated 5WTi(C)(pH 10, 550 °C) and model impregnated supported 5WTi(I)(550 °C) catalysts.

also corresponds to the symmetric stretch of dehydrated surface mono-oxo $O=WO_4$ species as shown by ^{18}O–^{16}O exchange. The difference between the two surface mono-oxo $O=WO_4$ species is related to their extent of oligomerization [23]. The Raman band at ~983–986 cm^{-1} corresponds to smaller surface mono-oxo $O=WO_4$ oligomers that may be trapped by surface defects apparently introduced by the co-precipitation synthesis [61]. The low number of surface defects on the reference TiO_2 support (P25, Evonik/Degussa) is related to the very high temperatures (~1000–1100 °C) of its synthesis [62] that tends to anneal the surface defects. The relative concentration of the surface $O=WO_4$ (982–984 cm^{-1})/$O=WO_4$ (1012–1014 cm^{-1}) sites increases slightly with synthesis pH. The low XANES pre-edge energy for the dehydrated supported co-precipitated WO_3-TiO_2 catalysts further reflects the $WO_{5/6}$ coordination of the surface $O=WO_4$ species [15]. The absence of detectable $^{18}O=W=^{16}O$ bands at 1925–1975 cm^{-1} during the oxygen exchange confirms the surface mono-oxo $O=WO_4$ structures for both sites.

The rapid oxygen exchange of the W=O bonds with $H_2{}^{18}O$ vapor at elevated temperatures and the sluggish oxygen exchange of the TiO_2 support demonstrates that the WO_x sites are present on the outer surface of the TiO_2 support. Thus, the proposal that co-precipitated catalysts may also contain tungsten oxide in the titania interlayer spaces [1,3,6], which has never been backed up with supporting data, is not supported by the new findings. The high mobility of tungsten oxide at temperatures of 550–700 °C further argues against the stabilization of WO_x in the titania interlayer spaces and its segregation to the surface of TiO_2 particles

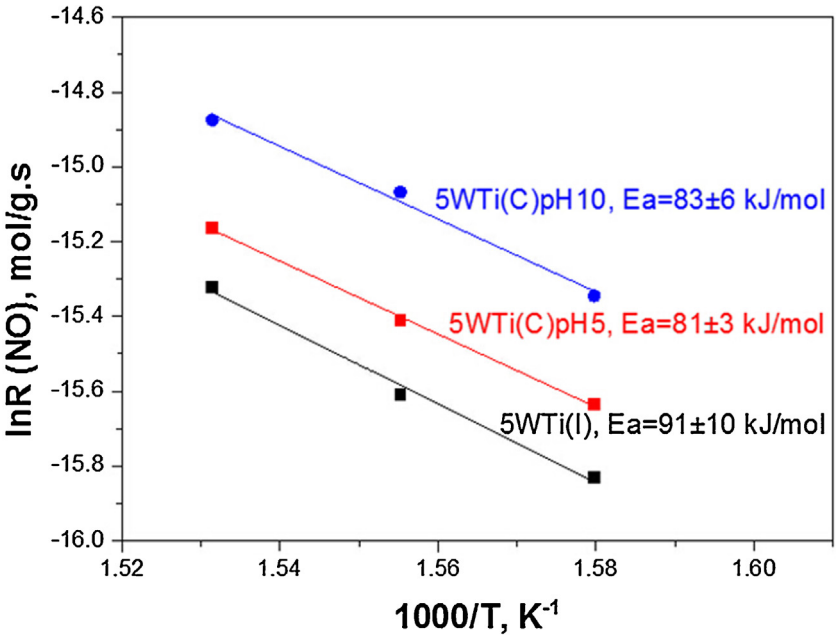

Fig. 6. Steady-state $NO/NH_3/O_2$ SCR reaction rates as a function of temperature (1/T) for the co-precipitated 5WTi(C) (pH 5, 550 °C), co-precipitated 5WTi(C) (pH 10, 550 °C) and impregnated supported 5WTi(I) (550 °C) catalysts.

because of the low surface-free energy of tungsten oxide [63]. It may, however, be possible that a minor amount of WO_x is trapped in the titania interlayer spaces. The miniscule amounts and the inaccessibility of such potential sites to NO and NH_3 suggest that they would not have a catalytic effect on the NO/NH_3 SCR reaction. The previous proposal of supported $(WO_x)_3$ clusters on the co-precipitated WO_3-TiO_2 catalyst, with assignment of the vibrations at ~980 cm^{-1} resulting from W = O sites with predominantly W-O-Ti linkages to the titania support ("inner" sphere) and above 1005 cm^{-1} associated with W = O sites from surface WO_x on top of the titania-supported tungsten oxide domains ("outer" sphere) [15] has no supporting data since $(WO_3)_3$ trimers supported on nanoporous WO_3 only give rise to one IR band at 1022 cm^{-1}. [64] This assignment is also not consistent with the characteristics of the well-established surface mono-oxo $O=WO_4$ sites anchored to the titania support for the model supported WO_x/TiO_2 catalyst that only give rise to one Raman band (~1016 cm^{-1}) and one IR overtone band (~2020 cm^{-1}).

The extent of oligomerization of each surface $O=WO_4$ site with surface coverage is not strongly dependent on the synthesis pH conditions since the vibrational shifts for the two distinct surface $O=WO_4$ species with surface coverage are minor (only ~2 cm^{-1} in their Raman spectra) for both sites on the co-precipitated catalysts calcined at 550 °C. The extent of oligomerization of each surface $O=WO_4$ site, however, becomes slightly greater (~5 cm^{-1}) as the calcination temperature is increased to higher temperatures due to decreasing surface area of the titania support with temperature (see Fig. S1).

The industrial patents propose that at controlled alkaline pH values certain surface −OH hydroxyls form on the co-precipitated WO_3-TiO_2 powders that prevent aggregation of tungsten oxide on the TiO_2 support for the preparation scale employed for industrial production [35–37]. This proposal is not supported by the present lab-scale studies with 5% WO_3 catalysts since all the tungsten oxide species are completely dispersed as surface mono-oxo $O=WO_4$ species on TiO_2 independent of solution pH employed in the synthesis and anchor at isolated surface Ti-OH sites. The use of controlled alkaline solutions, however, may still be important for higher tungsten oxide loadings and industrial-scale production of co-precipitated WO_3-TiO_2 powders.

4.2. Thermal stability of WO_3-TiO_2 catalysts

The thermal stability of the co-precipitated WO_3-TiO_2 catalysts is poor since about half of their surface area is lost when the calcination temperature is increased from 550 to 700 °C independent of synthesis pH (see Table 1). The loss in surface area increases the surface WO_x density and, consequently, increases the extent of polymerization of the surface $O=WO_4$ species (Raman shift of ~5 cm^{-1}; see Fig. S4). These calcination temperatures, however, are significantly in excess of typical selective catalytic reduction (SCR) operating conditions of 300–400 °C, but the trend may be important for long term industrial use. Importantly, the surface $O=WO_4$ sites on all the co-precipitated and reference impregnated catalysts were thermally stable upon calcination at elevated temperatures since crystalline WO_3 NPs were not formed. The surface $O=WO_4$ sites also retard the sintering of the TiO_2 support as revealed by the significant decrease in surface area of the reference TiO_2 support in the absence of surface WO_x species upon calcination at elevated temperatures compared to the model supported 5% WO_x/TiO_2 catalyst (see Table 1). Thus, a synergistic interaction exists between the surface WO_x sites and the TiO_2 support that stabilizes both components at elevated temperatures.

4.3. Surface acidity of WO_3-TiO_2 catalysts

The TiO_2 support only contains surface Lewis acid sites and Brønsted acid sites only form upon the addition of surface transition metal oxides [65]. As the synthesis pH is increased for the co-precipitated catalysts, the amounts of surface Brønsted acid sites decrease and surface Lewis acid sites increase. This leads to a decrease in the B/L ratio with increasing synthesis pH. The amounts of both types of surface acid site increases with calcination temperature and track the oligomerization of the surface WO_x sites. The model supported 5% WO_x/TiO_2 catalyst most closely resembles the acidity of the co-precipitated catalyst prepared at pH = 10. These

trends in surface acidity will be compared with the corresponding reactivity studies below.

4.4. Structure-activity relationships for $NO/NH_3/O_2$ SCR by WO_3-TiO_2 catalysts

All the tungsten oxide-titania catalysts contain the surface O=WO_4 site giving rise to the symmetric vibration at ~1010–1016 cm^{-1} (IR overtone at ~2017 cm^{-1}) and the co-precipitated WO_3-TiO_2 catalysts also possess a second mono-oxo O=WO_4 site giving rise to its symmetric stretch at ~983 cm^{-1} (IR overtone at ~1992–2000 cm^{-1}). The new surface WO_x site for the co-precipitated catalyst is thought to be associated with the presence of defects of the co-precipitated titania support, and the concentration of these defects increases with the synthesis pH. The concentration of the new surface WO_x sites on the co-precipitated titania supports, however, is only a minor fraction of the total surface WO_x sites.

The new surface WO_x sites and associated titania defects influence the surface chemistry of the co-precipitated catalysts. The amount of adsorbed ammonia is increased for the co-precipitated catalysts. The new surface WO_x sites exhibit an enhanced low temperature NO/NH_3-TPSR peak at ~340 °C and lower the steady-state SCR activation energy by ~10 kJ/mol corresponding to a modest increase in TOF values: 5WTi(pH 10, 550 °C) > 5WTi(pH 5, 550 °C) > 5WTi(I, 550 °C). The slight increase of the SCR activity for the co-precipitated 5WTi(pH 5) catalyst relative to the 5WTi(I) catalyst and the enhanced SCR activity of the 5WTi(pH 10, 550 °C) catalyst suggests that there may be other aspects of the co-precipitated catalysts that are still not fully understood. Although the overall influence of the co-precipitation on WO_3-TiO_2 catalysts is modest, only a factor of ~2 in SCR specific activity, such minor changes and the enhanced ammonia adsorption capacity may have important implications for SCR with V_2O_5-WO_3-TiO_2 catalysts. The influence of the co-precipitation synthesis on V_2O_5-WO_3-TiO_2 catalysts will be addressed in a subsequent publication.

5. Conclusions

A series of co-precipitated WO_3-TiO_2 catalysts, prepared at different pH values, was compared with a conventional impregnated supported WO_x/TiO_2 catalyst. The model supported WO_x/TiO_2 catalyst only contained one surface mono-oxo O=WO_4 site (~1016 cm^{-1}) while the co-precipitated catalysts possessed the same mono-oxo site (~1012–1014 cm^{-1}) as well as a new surface mono-oxo O=WO_4 site (~983–985 cm^{-1}). The new site only represents a minor fraction of the total surface WO_x sites. The new mono-oxo O=WO_4 site is thought to be associated with surface defects of the titania support. In general, the co-precipitated catalysts possessed higher surface area and greater amounts of surface Brønsted acid sites, but these parameters did not correlate with the SCR activity. The co-precipitated catalysts exhibited higher reactivity during $NO/NH_3/O_2$-SCR and NO/NH_3-TPSR suggesting that the new surface WO_x sites and surface defects are responsible for the increased activity. The enhanced activity with increasing synthesis pH is not fully understood and suggests that additional contributing factors may also be affecting the SCR activity. The findings confirm the patent literature claim that co-precipitated catalysts prepared at high pH give improved SCR activity, but this is not due to better dispersion of the surface tungsten oxide phase on the titania support as claimed. It is important to first be familiar with the structure-activity of the co-precipitated WO_3-TiO_2 catalysts to better understand the structure-activity of co-precipitated V_2O_5-WO_3-TiO_2 SCR catalysts, which will be the subject of a following study.

Acknowledgments

Ms. Yuanyuan He is grateful for financial support from the China Scholarship Council (CSC) for the State Scholarship and National Natural Science Funds of China (Nos. 51274263 and 51204220). Prof. I.E. Wachs (Lehigh University), M. Zhu (Lehigh) and Dr. Zili Wu (Oak Ridge National Laboratory) were supported by the Center for Understanding & Control of Acid Gas-Induced Evolution of Materials for Energy (UNCAGE-ME), an Energy Frontier Research Center funded by DOE, Office of Science, Office of Basic Energy Sciences under grant DE-SC0012577. A portion of this research including the isotopic exchange was conducted at the Center for Nanophase Materials Sciences, which is a DOE office of the Science User Facility. The authors thank D. G. Gregory and Ms. Q. Guo of Lehigh University for experimental assistance in obtaining BET and BJH data. DGG is also thanked for assistance in obtaining the XRD spectra. Dr. Henry Luftman of Lehigh University is thanked for collecting the HS-LEIS data.

Appendix A. Supplementary data

Supplementary data associated with this article can be found, in the online version, at http://dx.doi.org/10.1016/j.apcatb.2016.01.072.

References

[1] L. Lietti, J. Svachula, P. Forzatti, G. Busca, G. Ramis, F. Bregani, Catal. Today 17 (1993) 131–139.
[2] M. Kobayashi, K. Miyoshi, Appl. Catal. B 72 (2007) 253–261.
[3] G. Busca, L. Lietti, G. Ramis, F. Berti, Appl. Catal. B 18 (1998) 1–36.
[4] S. Meijers, L.H. Gielgens, V. Ponec, J. Catal. 156 (1995) 147–153.
[5] J. Macht, R.T. Carr, E. Iglesia, J. Catal. 264 (2009) 54–66.
[6] P. Patrono, A. Laginestra, G. Ramis, G. Busca, Appl. Catal. A 107 (1994) 249–266.
[7] Y.T. Kwon, K.Y. Song, W.I. Lee, G.J. Choi, Y.R. Do, J. Catal. 191 (2000) 192–199.
[8] C. Martin, G. Solana, V. Rives, G. Marci, L. Palmisano, A. Sclafani, Catal. Lett. 49 (1997) 235–243.
[9] S.M. Lee, S.S. Kim, S.C. Hong, Chem. Eng. Sci. 79 (2012) 177–185.
[10] M.D. Amiridis, R.V. Duevel, I.E. Wachs, Appl. Catal. B 20 (1999) 111–122.
[11] P. Forzatti, Appl. Catal. A 222 (2001) 221–236.
[12] S. Djerad, L. Tifouti, M. Crocoll, W. Weisweiler, J. Mol. Catal. A: Chem. 208 (2004) 257–265.
[13] E.I. Ross-Medgaarden, I.E. Wachs, W.V. Knowles, A. Burrows, C.J. Kiely, M.S. Wong, J. Am. Chem. Soc. 131 (2009) 680–687.
[14] A. Scholz, B. Schnyder, A. Wokaun, J. Mol. Catal. A: Chem. 138 (1999) 249–261.
[15] S. Eibl, B.C. Gates, H. Knozinger, Langmuir 17 (2001) 107–115.
[16] I.E. Wachs, T. Kim, E.I. Ross, Catal. Today 116 (2006) 162–168.
[17] E.I. Ross-Medgaarden, I.E. Wachs, J. Phys. Chem. C 111 (2007) 15089–15099.
[18] T. Onfroy, V. Lebarbier, G. Clet, M. Houalla, J. Mol. Catal. A: Chem. 318 (2010) 1–7.
[19] G.D. Panagiotou, T. Petsi, K. Bourikas, C. Kordulis, A. Lycourghiotis, J. Catal. 262 (2009) 266–279.
[20] I. Giakoumelou, C. Fountzoula, C. Kordulis, S. Boghosian, J. Catal. 239 (2006) 1–12.
[21] A. Gutierrez-Alejandre, P. Castillo, J. Ramirez, G. Ramis, G. Busca, Appl. Catal. A 216 (2001) 181–194.
[22] J. Engweiler, J. Harf, A. Baiker, J. Catal. 159 (1996) 259–269.
[23] T. Kim, A. Burrows, C.J. Kiely, I.E. Wachs, J. Catal. 246 (2007) 370–381.
[24] J.R. Sohn, J.H. Bae, Korean J. Chem. Eng. 17 (2000) 86–92.
[25] F.B. Li, G.B. Gu, X.J. Li, H.F. Wan, Acta Phys. Chim. Sin. 16 (2000) 997–1002.
[26] X.F. Yu, N.Z. Wu, H.Z. Huang, Y.C. Xie, Y.Q. Tang, J. Mater. Chem. 11 (2001) 3337–3342.
[27] New frontiers in catalysis, in: F. Hilbrig, H. Schmelz, H. Knözinger, L. Guzci, F. Sosymosi, P. Tetenyi (Eds.), Proceedings of the 10th International Congress on Catalysis, Budapest, Hungary, July 19–24, 1992, Elsevier, Amsterdam, 1993, pp. 1351–1362.
[28] W.Q. Liu, X.H. Liu, J.Y. Zhang, J. Petrochem. Univ. 1 (2003) 1–4.
[29] V. Lebarbier, G. Clet, M. Houalla, J. Phys. Chem. B 110 (2006) 22608–22617.
[30] X.Z. Li, F.B. Li, C.L. Yang, W.K. Ge, J. Photochem. Photobiol. A 141 (2001) 209–217.
[31] H.M. Yang, R.R. Shi, K. Zhang, Y.H. Hu, A.D. Tang, X.W. Li, J. Alloys Compd. 398 (2005) 200–202.
[32] F.C. Jentoft, H. Schmelz, H. Knozinger, Appl. Catal. A 161 (1997) 167–182.
[33] K.K. Akurati, A. Vital, J.P. Dellemann, K. Michalow, T. Graule, D. Fetti, A. Baiker, Appl. Catal. B 79 (2008) 53–62.

[34] M.A. Reiche, T. Burgi, A. Baiker, A. Scholz, B. Schnyder, A. Wokaun, Appl. Catal. A 198 (2000) 155–169.
[35] Y. Qiu, F. Zeng, G. Liang, H. Xu, X. Wu, Z. Chen, J. Qin, Q. Lu, H. Liao, Method for Preparation of Specific Ti-W Powder for SCR (selective catalytic reduction) Denitrification Catalyst, CN 102764662, 2012.
[36] L. Wang, Z. Li, Q. Zhang, Method for Preparation of Titania-Tungsten Trioxide Composite Powder as Denitrification Catalyst Support, CN 102327783, 2012.
[37] L. Mitsubishi, Heavy Industries, Calcined Titania-Tungsten and/or Molybdenum Oxide(s) as a Flue Gas Denitration Catalyst or its Support, Jpn. Kokai Tokkyo Koho JP 59035026A, 1984.
[38] F. Hilbrig, H. Schmelz, H. Knozinger, M. Sinev, A.T. Bell, M. Schmal, P. Forzatti, I.E. Wachs, T. Uematsu, J.C. Vedrine, E. Hums, Stud. Surf. Sci. Catal. 75 (1993) 1351–1362.
[39] I.R. Beattie, T.R. Gilson, J. Chem. Soc. (A) (1969) 2322-2327; Proc. R. Soc. London, Ser. A 307 (1968) 407–429.
[40] G. Madia, M. Elsener, M. Koebel, F. Raimondi, A. Wokaun, Appl. Catal. B 39 (2002) 181–190.
[41] M.A. Vuurman, I.E. Wachs, A.M. Hirt, J. Phys. Chem. 95 (1991) 9928–9937.
[42] F. Hilbrig, H.E. Gobel, H. Knozinger, H. Schmelz, B. Lengeler, J. Phys. Chem. 95 (1991) 6973–6978.
[43] J.A. Horsley, I.E. Wachs, J.M. Brown, G.H. Via, F.D. Hardcastle, J. Phys. Chem. 91 (1987) 4014–4020.
[44] L. Nakka, J.E. Molinari, I.E. Wachs, J. Am. Chem. Soc. 131 (2009) 15544–15554.
[45] G. Deo, A.M. Turek, I.E. Wachs, T. Machej, J. Haber, N. Das, H. Eckert, A.M. Hirt, Appl. Catal. A 91 (1992) 27–42.
[46] D.S. Kim, M. Ostromecki, I.E. Wachs, J. Mol. Catal. A: Chem. 106 (1996) 93–102.
[47] M.M. Ostromecki, L.J. Burcham, I.E. Wachs, J. Mol. Catal. A: Chem. 132 (1998) 59–71.
[48] E.L. Lee, I.E. Wachs, J. Phys. Chem. C 111 (2007) 14410–14425.
[49] M. Baron, H. Abbott, O. Bondarchuk, D. Stacchiola, A. Uhl, S. Shaikhutdinov, H.J. Freund, C. Popa, M.V. Ganduglia-Pirovano, J. Sauer, Angew. Chem. Int. Ed. 48 (2009) 8006–8009.
[50] A. Gutierrez-Alejandre, J. Ramirez, G. Busca, Langmuir 14 (1998) 630–639.
[51] G. Ramis, G. Busca, C. Cristiani, L. Lietti, P. Forzatti, F. Bregani, Langmuir 8 (1992) 1744–1749.
[52] G. Busca, J. Raman Spectrosc. 33 (2002) 348–358.
[53] G.A. Tompsett, G.A. Bowmaker, R.P. Cooney, J.B. Metson, K.A. Rodgers, J.M. Seakins, J. Raman Spectrosc. 26 (1995) 57–62.
[54] E.L. Lee, I.E. Wachs, J. Phys. Chem. C 112 (2008) 6487–6498.
[55] L. Lietti, J.L. Alemany, P. Forzatti, G. Busca, G. Ramis, E. Giamello, F. Bregani, Catal. Today 29 (1996) 143–148.
[56] J.M.G. Amores, V.S. Escribano, G. Ramis, G. Busca, Appl. Catal. B 13 (1997) 45–58.
[57] L. Lietti, I. Nova, S. Camurri, E. Tronconi, P. Forzatti, AlChE J. 43 (1997) 2559–2570.
[58] N.Y. Topsoe, J.A. Dumesic, H. Topsoe, J. Catal. 151 (1995) 241–252.
[59] N.Y. Topsoe, H. Topsoe, J.A. Dumesic, J. Catal. 151 (1995) 226–240.
[60] T. Nakata, S. Matsushi, J. Phys. Chem. 72 (1968) 458–464.
[61] Y. Li, Z.H. Wei, F. Gao, L. Kovarik, C.H.F. Peden, Y. Wang, J. Catal. 315 (2014) 15–24.
[62] L. White, G. Duffy, Ind. Eng. Chem. 51 (1959) 232–238.
[63] C.B. Wang, Y.P. Cai, I.E. Wachs, Langmuir 15 (1999) 1223–1235.
[64] Z.J. Li, B. Smid, Y.K. Kim, V. Matolin, B.D. Kay, R. Rousseau, Z. Dohnalek, J Phys Chem Lett 3 (2012) 2168–2172.
[65] J. Datka, A.M. Turek, J.M. Jehng, I.E. Wachs, J. Catal. 135 (1992) 186–199.